Response to Reviewers

The authors greatly acknowledge the anonymous reviewer for carefully reading the manuscript and providing constructive comments. This document contains the author's responses. Each comment is discussed separately with the following typesetting:

Reviewer's comments

Authors response

Changes in the manuscript

The manuscript presents ambient measurements of Saharan dust intrusions at ground level in Southern Spain. The polarized imaging nephelometer enables the measurement of the phase function and polarized phase function and at several wavelengths at scattering angles between 5° and 175°. Especially the polarized phase function is an important quantity in passive remote sensing. They could show with their spectral measurements, that the polarized phase function behaves similar in the observed wavelength range (405 till 660 nm) for intense dust events. Whereas dust which was mixed with local pollution shows a different spectral behavior, especially at the shortest wavelength of 405 nm. Additionally, simulated (polarized) phase functions are shown. However, I see that for a publication in ACP, the research findings should be set into a broader context and the novelty of the study should be worked out stronger. After addressing my comments below, and please take my major comments serious, a publication in ACP can be recommended.

We thank the reviewer for the comments addressed that helped to improve the quality of the manuscript. Also, following the suggestion of other referees, we have re-written the abstract to highlight the objective and findings of our manuscript

This work investigates the scattering matrix elements during different Saharan dust outbreaks over Granada (South-East Spain) in 2022 using the Polarized Imaging Nephelometer (PI-Neph PIN100, GRASP-Earth). The PI-Neph is capable of measuring continuously the phase function (F_{11}) and the polarized phase function ($-F_{12}/F_{11}$) at three different wavelengths (405, 515 and 660 nm) in the range 5° - 175° with 1° resolution for ambient aerosol samples. Extreme dust events ($PM_{10} > 700$ μgm^{-3}) occurring in March 2022 are compared with more frequent and moderate events registered in summer 2022 (PM_{10} between 50 and 100 μgm^{-3}). These intercomparisons allow the evaluation of F_{11} and $-F_{12}/F_{11}$ when dust particles predominate in the aerosol sample, but also when there is a possible mixture with other anthropogenic particles. For F_{11} there are no remarkable differences between extreme and moderate events. However, results of $-F_{12}/F_{11}$ show differences between extreme and moderate events: for 660 nm the $-F_{12}/F_{11}$ pattern is characterized by a bell-shape with a positive maximum in the 90º-120º scattering region, and this pattern is observed both in the extreme and moderate dust events. However, there are remarkable differences in $-F_{12}/F_{11}$ at 405 nm showing a very similar pattern with 660

nm during the peaks of the extreme dust events while for moderate events it shows a different pattern characterized by values around zero up to ~ 50°, decreasing later to negative values ~120° and increasing again to values close to zero in the backward scattering region. For 515 nm we found out intermedia patterns. The temporal evolutions during extreme dust events reveal that $-F_{12}/F_{11}$ at 405 nm is very sensitive to the particle concentrations. For the peak of the events, F_{11} and $-F_{12}/F_{11}$ agree with the laboratory measurements available in the Amsterdam-Granada Light Scattering database at all wavelengths. The combination of PI-Neph measurements with additional in-situ instrumentation allowed to obtain scattering (SAE) and absorption (AAE) Ångström exponents and to conduct a typing classification that revealed extreme dust events as pure dust, while moderate dust events were classified as a mixture of dust with urban background pollution. In addition, simulations with the Generalized Retrieval of Atmosphere and Surface Properties (GRASP) code explain the different patterns in $-F_{12}/F_{11}$ with changes in the refractive indexes and the contributions of the fine and coarse mode. Therefore, our results confirm that differences in the phase matrix elements of Saharan dust outbreaks of varying intensity can be explained by the mixing conditions of dust with the background particles.

And we have also modified the introduction section to better contextualize our manuscript (L83-158):

Remote sensing techniques are widely used to infer dust properties. For example, passive remote sensing techniques such as sun-photometry by the Aerosol Robotic Network (AERONET – (Holben et al., 1998)) or star/moon photometry (i.e Pérez-Ramírez et al., 2008, Pérez-Ramírez et al., 2011;Berkoff et al., 2011) allow to have a representation of column-integrated values, particularly aerosol optical depth (AOD). But to infer other aerosol optical (e.g. aerosol complex refractive index and single scattering albedo) and microphysical (e.g. aerosol size distribution) properties it is necessary to solve ill-posed problems where the information content is low (Dubovik & King, 2000; King et al., 1978; Nakajima et al., 1996; Olmo et al., 2006, 2008; Pérez-Ramírez et al., 2015). These algorithms use the Mie theory for the internal computation of particles phase functions, but in the case of dust particles more complex approaches such as T-Matrix are needed because of the non-sphericity of dust particles (Mischenko & Travis, 1994, 1997) . Nevertheless, several inversion algorithms have been developed incorporating T-Matrix modeling, being one of the most popular algorithms developed within the AERONET network (Dubovik et al., 2006).

Ground-based remote sensing techniques are only representative of the measurement site, and to face these limitations satellite measurements are ideal because they can cover wide regions of the world. However, passive remote sensing space platforms deal with additional complexity in the retrieval of aerosol properties because of the influence of surface reflectance (Kahn et al., 1998; Levy et al., 2007). The simplest retrievals use look-up tables with a priori aerosol types with great success in obtaining AOD, but limited capacity for obtaining other aerosol parameters because of the difficulties to separate the signals corresponding to the atmosphere and surface (Dubovik et al., 2019). To solve these limitations, the use of multiwavelength and multi-angle polarization measurements is ideal to improve the information content (Mishchenko et al., 2007). Some of the first polarized-based measurements for aerosol studies were carried out by the POLDER

instrument (POlarization and Directionality of the Earth's Reflectances – (Deuzé et al., 1993)) that acquired 9 years of data. These measurements were used as inputs in the Generalized Retrieval of Atmosphere and Surface Properties algorithm (GRASP – (Dubovik et al., 2014, 2021)) for obtaining extended aerosol optical and microphysical properties. Algorithms such as GRASP are becoming the operational algorithms in new satellite missions (Remer et al., 2019; Fuertes et al., 2022; Hasekamp et al., 2024), but these algorithms need phase matrix measurements that allows the optimization of the kernels used internally, particularly for non-spherical particles.

The main difficulties for measuring aerosol phase matrix of ambient air are in the design and development of appropriate polar nephelometry capable of measuring light scattered with appropriate angular resolution. The first polar nephelometry developments were based on moveable detectors, but they must be mechanically stable and require a constant population of aerosol particles that does not change appreciably during the detector sweep (Holland & Gagne, n.d.; Hovenier et al., 2003; Jaggard et al., 1981; Kuik et al., 1991; Perry et al., 1978; Volten et al., 2001a). Other polar nephelometry designs use arrays of many detectors placed on representative scattering angles (Barkey et al., 1999; Gayet et al., 1998; Pope et al., 1992; West et al., 1997; Wyatt et al., 1988), but this technique requires careful calibration of the detectors and generally suffers from low angular resolution (~2º). Those instrumental limitations have implied that the usual study of scattering matrix elements of dust particles were done in the laboratory for synthetic samples minerals that compose dust particles (Curtis et al., 2008; Huang et al., 2020; Meland et al., 2010; Muñoz et al., 2010a; J. B. Renard et al., 2014; J.-B. Renard et al., 2010) or with collected dust samples (Muñoz et al., 2007a; J. B. Renard et al., 2014; J.-B. Renard et al., 2010, 2024). Actually, the parametrizations of mineral dust phase matrix used for AERONET algorithm were calculated by fitting the laboratory measurements of different non-spherical particles samples (i.e. Dubovik et al., 2006). Such measurements were performed at a few wavelengths, and what is more important, they might be non-representative of real aerosol measurements because of the different transformations and interactions of dust particles since they are emitted in their source regions. There is therefore a current challenge in having an extended database of measurements of dust phase matrix elements for different dust types and mixtures.

The latest developments in polar nephelometry use imaging techniques (Bian et al., 2017; Curtis et al., 2007; Dolgos & Martins, 2014) to determine phase matrix with single detector and relatively compact design that does not require moveable parts. The Polarized Imaging Nephelometer (PI-Neph) was one of the first designs of a polar nephelometer that used imaging techniques, developed by the University of Maryland, Baltimore County (UMBC). This first prototype of the PI-Neph could acquire aerosol phase matrix at 473, 532 and 671 nm with 0.5º resolution. The instrument was deployed on the NASA DC8 aircraft and operated during special field campaigns (Espinosa et al., 2018; Reed Espinosa et al., 2017). Other PI-Neph instruments based on the first UMBC design are operated by NOAA (Ahern et al., 2022; Manfred et al., 2018). The main novelty of these prototypes is that they measure phase matrix elements of ambient air, where conditions can be very different to laboratory measurements. However, to date none of these instruments have been operating continuously and reported any multiwavelength measurements of Saharan dust. The imaging technique is being expanded worldwide with further designs although limited to laboratory operation yet

(Moallemi et al., 2023). All designs in polar nephelometry present physical limitations that limit the measurements to the range 3º-178º, but synthetic tests have revealed that multi-wavelength polarimetric PI-Neph measurements improve the information content for the retrieval of aerosol optical and microphysical properties (Moallemi et al., 2022) . Therefore, measurements of dust phase matrix elements for ambient aerosol samples in the atmosphere will serve to further advance in the understanding of mineral dust absorption properties and chemical composition (Di Biagio et al., 2017, 2019).

This work presents phase matrix measurements of ambient Saharan dust particles by the GRASP-Earth's (https://www.grasp-earth.com/) multi-wavelength PI-Neph. The instrument was developed using the heritage of previous PI-Neph developments made by UMBC and can provide aerosol phase matrix elements at 405, 515 and 660 nm of ambient samples in the range 5° - 175° with 1° resolution. Measurements were acquired in the urban background station (UGR) of the Andalusian Global ObseRvatory of the Atmosphere (AGORA) located in the Southeast of the Iberian Peninsula where the main source of natural particles is the Sahara Desert's transported particles (Querol et al., 2019). We present the results for extreme outbreaks that occurred in March 2022 (Rodríguez & López-Darias, 2024) with PM_{10} (particulate matter with diameter < 10 µm) concentrations over 700 μgm^{-3}, and for more typical situations of moderate dust events with PM_{10} concentrations ~100 μgm^{-3}. The measurements presented of the phase matrix for Saharan dust are unique and are and step forward from the ancillary measurements performed in the region by Horvath et al., (2018) with a single wavelength polar nephelometry (no polarization was available)."

Major comments:

The paper would benefit a lot, if you include lidar observations to your dust cases. I know that the University of Granada operates a polarization lidar (otherwise I would not ask for it) which could clearly show the Saharan dust layers above the station (Sect. 3.1). Additionally, it may provide you with directly measured lidar ratios. Then, there is just the gap between the PI Nephelometer observations at the ground and the lidar measurements in the lofted Saharan dust layers. So please include your colleagues from the lidar group with their lidar observations at UGR.

-We agree with the reviewer that PI-Neph measurements can complement lidar measurements available in the University of Granada station. The lidar system in our station (MULHACEN) is part of the EARLINET/ACTRIS network. We have been continuously in contact with our colleagues that are in charge of the lidar system MULHACEN and there are several reasons why such kind of measurements are not included in the present manuscript.

The main reason is the lack of appropriate lidar signals during the extreme Saharan dust outbreaks. We include in the Figure below (Figure R1) the temporal evolution of lidar Range Corrected Signal (RCS) at 532 nm. The RCS reveals that the main aerosol layers are found below 1.5 km approximately. However, when analyzing these RCS we found out that they were saturated and no retrievals of backscattering and extinction coefficients were possible. Moreover, our lidar system had a large region of incomplete overlap from

the ground up to 1.3km, and thus the intense dust layer could not have been monitored even if signals would not have been saturated. Actually, only one profile fulfilled data quality criterion of EARLINET single calculus chain, and the results are illustrated here in Figure R2.

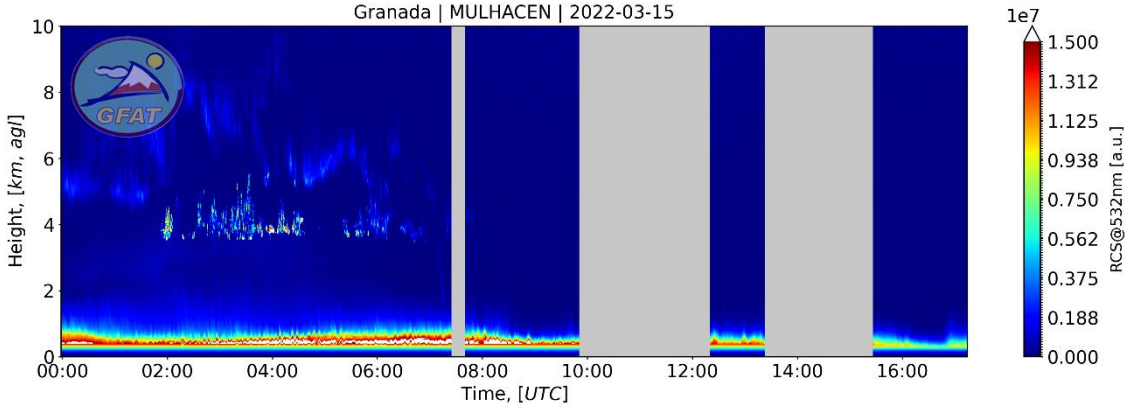

Figure R1: Temporal evolution of the Range Corrected Signal (RCS) at 532 nm on 15th March 2022 in the EARLINET/ACTRIS lidar system operating in AGORA.

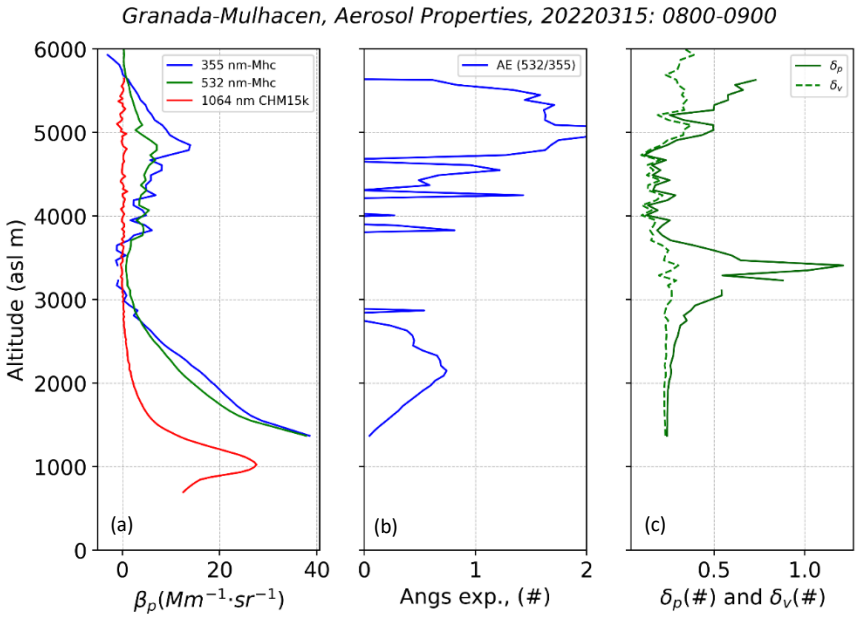

Figure R2: Vertical profiles of (a) aerosol backscattering coefficient at 355 and 532 nm obtained with the MULHACEN system plus that at 1064 nm obtained with a CHM15k Ceilometer – that assumes constant lidar ratio (b) backscattering Angström Exponent (AE) between 532 and 355 nm and (c) particle and volume depolarization.

The profiles of Figure R2 clearly show the lack of capacity for obtaining aerosol properties below 1.3 km approximately. Retrieval of backscattering at 355 nm seems to reach negative values above 5.5 km approximately that suggest the difficulties of finding a good signal in the clean zone, which is needed in the lidar retrieval. These difficulties in the retrieval can be behind the noisy retrievals of AE, but even though AE values above 4 km did not reveal large dependence of coarse particles. Moreover, the values of δp and δv do not correspond with values of large dominance of coarse particles, agreeing with AE values. Therefore, the lidar measurements by the MULHACEN system on 15th March

2022 were not useful to complement the PI-Neph measurements at surface. For the case on 25th March we found very similar situation, as the RCS at 532 nm show in Figure R3

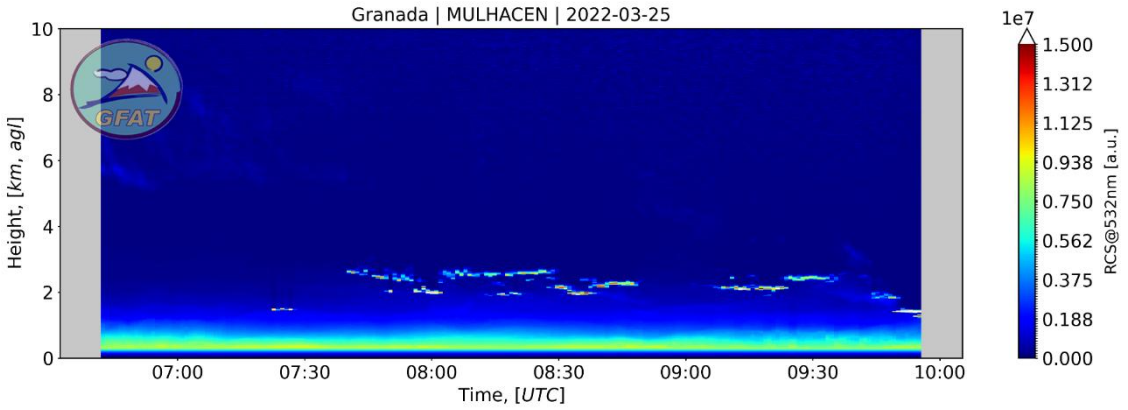

Figure R3: Temporal evolution of the Range Corrected Signal (RCS) at 532 nm on 25th March 2022 in the EARLINET/ACTRIS lidar system operating in AGORA.

For the rest of PI-Neph data shown in Figure 8 there are certainly some correlative MULHACEN measurements. But the main limitation is in the large zone of incomplete overlap for the MULHACEN system that as commented include always the first kilometer (in some cases up to 1.5 km from the ground). That makes not possible a direct comparison between lidar ratios obtained by the two instruments. Only cases with very well mixed conditions could serve in those comparisons.

The main objective of this study is to discuss similitudes and differences of aerosol phase matrix for two extreme Saharan dust outbreaks versus those obtained during more frequent intrusions in the AGORA stations. The measurements with the PI-Neph are in the range 5-175º which is a very wide range, while lidar measurements only refer to values exactly at 180º. Thus, we believe that the lack of appropriate lidar measurements for intercomparisons does not affect the overall objective of our study. Nevertheless, we are aware of the benefit of lidar measurements with phase matrix measurements with the PI-Neph. In this sense, the research team of the AGORA station is implementing the appropriate approach to make the intercomparisons between LRs obtained by PI-Neph and those by lidar. To do so, a special field campaign called LUMINOUS was carried out in summer 2024. LUMINOUS was partly funded by ACTRIS Transnational Access and is an international cooperation between the University of Granada, the Paul Scherrer Institute (Switzerland) and GRASP-Earth. In LUMINOUS new designs of Inverse Multi-Angular Polarimeter with Polarization (IMAP - https://www.grasp-earth.com/imap/) were also deployed in the AGORA stations. One was in the UGR station (where MULHACEN operates) and the other in the Sierra Nevada station at 2.5 km altitude and at 20 km in straight line to the city of Granada. In LUMINOUS we operated other instruments for measuring particle size distribution and chemical compositions. The approach used in LUMINOUS avoids the problems of incomplete overlap and a direct intercomparisons between lidar and in-situ instruments in Sierra Nevada. At the moment, we are analyzing the first results from LUMINOUS.

In the present manuscript, the idea behind showing LRs in Figure 8 was to illustrate the variability of this parameter for different mixtures of mineral dust and

anthropogenic particles. After the referee questions, we believe that this was not emphasized in the manuscript and have modified the text to highlight this variability, and that further analysis is needed that incorporates also lidar measurements. This has been clarified in the revised manuscript when defining LRs computations using PI-Neph data. Also, we highlight that the exact measurements of $F_{11}(180º)$ required the use of specific instrumentation. Now between lines 265-270 is written:

The computation of $F_{11}(180°)$ has been made using the interpolation method used for completing the entire angular range in σ_{sca}. Other more robust methods can be used (i.e. Gomez-Martin et al., 2021), that can imply differences in $F_{11}(180°)$ of up to 20-30%. Therefore, LRs estimations will serve as an illustration of how this parameter varies under different conditions. We highlight that PI-Neph is not designed to accurately measure $F_{11}(180º)$ and there are other specific instruments that serve for that purpose (Järvinen et al., 2016; Miffre et al., 2023; Sakai et al., 2010).

In the discussion of the extreme event on 25th March 2022 we clarify that the data of LRs serve as an illustration of the mixture of particles (L406-407):

"Thus, the hypothesis that after 14:00 the presence of pollution particles becomes more relevant implies a decrease in SSA and illustrates variability in LRs, particularly in 405 nm."

Also, when discussing LRs for the entire period April-September 2022 we highlight that our results serve only as illustration of LRs variability (L554-566).

"The LR is a critical variable for backscattered lidar systems and is an intensive aerosol variable that strongly depends on $F_{11}(180°)$ and absorption (Pérez-Ramírez et al., 2019). Because of that, LRs can be very sensitive to the different mixtures of particles in the atmosphere (Burton et al., 2012, 2013; Müller et al., 2007). Results of Fig. 8 serve to illustrate LR variability for dusty conditions but with the influence of other types of particles. Generally, Fig. 8 shows values between 40 sr and 100 sr for the three wavelengths. The lower limits are closer to the values for large predominance of dust (i.e. Müller et al., 2007) while the upper values are typical values registered for predominance of smoke/anthropogenic particles (Alados-Arboledas et al., 2011b; Burton et al., 2012, 2013; Floutsi et al., 2023; Müller et al., 2007). Thus, results of Fig. 8 indicate the large sensitivity of LR to changes in the mixture of particles. A seasonal analysis indicates that in spring – although there is less data – LRs are above 75 sr with little spectral dependence, suggesting more influence of fine particles in the mixture, which are ultimately responsible for LR values. During the summer seasons the lower values around 40-50 sr are more frequent, suggesting more predominance of coarse particles in the mixture. "

The following references were added:

Alados-Arboledas, L., Müller, D., Guerrero-Rascado, J. L., Navas-Guzmán, F., Pérez-Ramírez, D., & Olmo, F. J. (2011a). Optical and microphysical properties of fresh biomass burning aerosol retrieved by Raman lidar, and star-and sun-photometry. *Geophysical Research Letters*, *38*(1). https://doi.org/https://doi.org/10.1029/2010GL045999

Burton, S. P., Ferrare, R. A., Hostetler, C. A., Hair, J. W., Rogers, R. R., Obland, M. D., Butler, C. F., Cook, A. L., Harper, D. B., & Froyd, K. D. (2012). Aerosol classification using airborne High Spectral Resolution Lidar measurements-methodology and examples. *Atmospheric Measurement Techniques*, *5*(1), 73–98. https://doi.org/10.5194/amt-5-73-2012

Burton, S. P., Ferrare, R. A., Vaughan, M. A., Omar, A. H., Rogers, R. R., Hostetler, C. A., & Hair, J. W. (2013). Aerosol classification from airborne HSRL and comparisons with the CALIPSO vertical feature mask. *Atmospheric Measurement Techniques*, *6*(5), 1397–1412. https://doi.org/10.5194/amt-6-1397-2013

Floutsi, A. A., Baars, H., Engelmann, R., Althausen, D., Ansmann, A., Bohlmann, S., Heese, B., Hofer, J., Kanitz, T., Haarig, M., Ohneiser, K., Radenz, M., Seifert, P., Skupin, A., Yin, Z., Abdullaev, S. F., Komppula, M., Filioglou, M., Giannakaki, E., … Wandinger, U. (2023). DeLiAn - a growing collection of depolarization ratio, lidar ratio and Ångström exponent for different aerosol types and mixtures from ground-based lidar observations. *Atmospheric Measurement Techniques*, *16*(9), 2353–2379. https://doi.org/10.5194/amt-16-2353-2023

Järvinen, E., Kemppinen, O., Nousiainen, T., Kociok, T., Möhler, O., Leisner, T., & Schnaiter, M. (2016). Laboratory investigations of mineral dust near-backscattering depolarization ratios. *Journal of Quantitative Spectroscopy and Radiative Transfer*, *178*, 192–208. https://doi.org/10.1016/j.jqsrt.2016.02.003

Miffre, A., Cholleton, D., Noël, C., & Rairoux, P. (2023). Investigating the dependence of mineral dust depolarization on complex refractive index and size with a laboratory polarimeter at 180.0 lidar backscattering angle. *Atmospheric Measurement Techniques*, *16*(2), 403–417. https://doi.org/10.5194/amt-16-403-2023

Pérez-Ramírez, D., Whiteman, D. N., Veselovskii, I., Colarco, P., Korenski, M., & da Silva, A. (2019). Retrievals of aerosol single scattering albedo by multiwavelength lidar measurements: Evaluations with NASA Langley HSRL-2 during discover-AQ field campaigns. *Remote Sensing of Environment*, *222*, 144–164. https://doi.org/10.1016/j.rse.2018.12.022

Sakai, T., Nagai, T., Zaizen, Y., & Mano, Y. (2010). *Backscattering linear depolarization ratio measurements of mineral, sea-salt, and ammonium sulfate particles simulated in a laboratory chamber*.

2. Do you have additional size distributions for your cases? The spectral slope of your scattering properties might depend on particle size. Having an additional size distribution would add certainly a lot of value to your discussion. Could you estimate the amount of pollution in your polarization measurements? It would be an important information in quantifying your observations. By requesting additional size distributions and lidar (lidar ratio) observations underlines my request to broaden your field and take all available information into account to deliver a comprehensive picture and to place your results in a broader context.

-We completely agree with the reviewer. Particle size distribution measurements would have solved many of the challenges in the analyses of aerosol phase matrix measurements. The AGORA observatory has an Aerosol Particle Sizer (APS TSI 3321) and an Aerosol Chemical Speciation Monitor (ACSM - Aerodyne). However, during the two extreme Saharan dust outbreaks in March 2022 these two instruments were not available to operate at the station due to maintenance tasks, that got extended until summer 2022. That is why these important measurements were not available for this study.

For the extreme event on 15th-16th March 2022 we measured the size distribution for the deposited dust (Figure R4). There is very low super-coarse mode if compared to the fine and coarse modes. Additionally, the modal radius of the coarse mode agrees with the aerosol size distribution used in GRASP simulations, which served as support to our simulations. This statement was added to the revised manuscript (L730-L731)

"The modal radii selected are close to those observed for the particle size distribution of the deposited particles in the UGR station (not shown for clarity)."

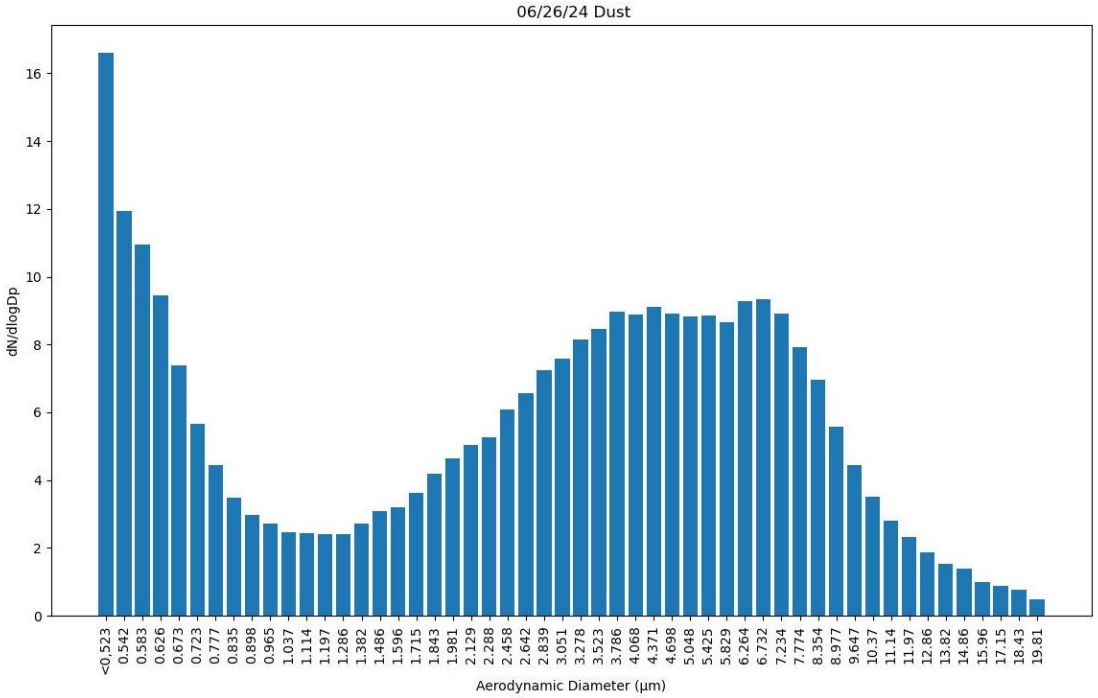

Figure R4. Number size distribution measured for the deposited dust for the extreme dust event on 15th – 16th March 2022.

The use of polarization measurement in GRASP also has a strong potential to differentiate pollution particles in the ambient samples affected by Saharan mineral dust. The challenge is optimizing GRASP to perform a retrieval capable of separating refractive index and other aerosol optical properties between fine and coarse mode. This is already available for the combination of backscattering lidar plus AERONET sun photometry measurements, but not for a configuration using only F_{11} and $-F_{12}/F_{11}$ as inputs. The simulations carried out only illustrate that the patterns observed in section 3.2.4 – now section 5.2 in the revised manuscript. Now, in the revised manuscript is given (L763-L768):

"However, studying the relationships between measured F_{11} and $-F_{12}/F_{11}$ with other aerosol optical and microphysical properties requires further analyses because F_{11} and $-F_{12}/F_{11}$ ultimately depend on the size distribution, refractive indexes, and particle shapes. The problem is even more complex if we differentiate optical properties between fine and coarse mode. Future optimization in GRASP will permit the retrieval of aerosol refractive indexes between fine and coarse mode separately using as inputs F_{11} and $-F_{12}/F_{11}$, and thus permitting further analyses of the different study cases discussed in this work."

Our group is collaborating with GRASP developers to implement such an approach in GRASP, and although preliminary results are promising, we need further analyses. Our goal is to prepare a future work with this new GRASP implementation and analyze our entire PI-Neph dataset – where we will analyze also cases not affected by Saharan dust particles.

Given the importance of the points raised by the referee (the other referees also pointed out very similar issues), we have decided to modify the conclusion section to emphasize the needs of acquiring correlative measurements of PI-Neph with additional instrumentation that provide information on particles size distribution and chemical compositions. Moreover, we emphasize the need for further advancing in GRASP for retrieving bimodal size distribution differentiating optical properties (especially refractive index) between fine and coarse modes using PI-Neph data (L849-864).

"Simulations performed by the GRASP code for different mixtures of fine mode (anthropogenic particles) and coarse mode (dust particles) revealed that F_{11} and $-F_{12}/F_{11}$ are sensitive to the different contribution of each mode in the mixture, being especially critical for $-F_{12}/F_{11}$ on the 405 nm channel. The negative values for $-F_{12}/F_{11}$ in 405 nm were observed more clearly for the mixture of fine and coarse particles. Thus, these simulations have served to understand the experimental negative values in $-F_{12}/F_{11}$ not observed in laboratory measurements for collected dust. Retrievals of bimodal size distribution with separate refractive indexes for each mode would have shown clarity to this problem. Hower, such retrieval with GRASP using F_{11} and $-F_{12}/F_{11}$ as inputs need to be optimized. Another additional optimization in GRASP will imply the possibility of implementing the retrieval of super-coarse mode particles. Nevertheless, the possibility of explaining the spectral differences in F_{11} and $-F_{12}/F_{11}$ with wavelength has served to understand the temporal evolution of the extreme dust events and the difference and similitudes when comparing versus laboratory measurements and versus other more moderate events of Saharan dust transport. However, going further in understanding the interaction of dust with these anthropogenic particles requires further analyses that provide the chemical composition and size distribution of the ensemble of particles and the final composition and shape of the particles after interacting. This is planned in future studies that will allow a more complete comprehensive analysis."

3. You have not written a lot concerning your uncertainty estimates. In Tab. 1 you provide uncertainties without mentioning what you are reporting. I guess, it is the standard deviation of the hourly mean, but it is stated nowhere. If it is the case, I am wondering about the systematic uncertainties of your measurements. Probably, it is reported elsewhere. But we need an assessment of the systematic uncertainties. Otherwise, the results are not comparable to other measurements.

-The reviewer is correct, the uncertainties in Table 1 correspond to the standard deviation of the hourly averages. We have added this information to the text (L422-423).

"Error bars in Table 1 are the standard deviations of the hourly mean values."

And modified Table 1 caption that now is given as (L513-516):

"Table 1. Hourly averaged properties of different stages of the extreme dust outbreaks in March 2022 reported in Figs. 6 and 7. The properties are reported at three wavelengths in the order of 660, 515 and 405 nm from top to bottom. Only the angular range of the PI-Neph (5°-175°) is used as the integration range of σ_{sca}. Error bars correspond to the standard deviations of the hourly means."

The issues about the uncertainties of the measurements have been also pointed out by the previous referee and by the comments of Jean-Baptiste Renard. In our previous study (Bazo et al., 2024), we performed an extensive characterization of the PI-Neph and error analyses. To avoid duplicate answer, we encourage the referee to read the overview of the study in Bazo et al., (2024) given to referee 1 – it should be published in the section public discussion. We highlight that in the new description of the PI-Neph we have given an overview of the error sources and uncertainties, plus the data quality check procedure. Now, between L199 and L225:

"An extensive analysis of the error sources in the PI-Neph was performed in Bazo et al., (2024) but an overview is given here: an exhaustive calibration of the instrument is performed consisting of two different steps. The first is a geometric correction that corrects from the different light paths to the different pixels in the CMOS camera. Later the absolute calibration permits to obtain phase matrix elements in physical units. In each step we used known scatterers (CO_2 and particle free air) whose parallel and perpendicular signals can be computed analytically using the Rayleigh theory (Anderson et al., 1996). Evaluation of the calibration with time did reveal great stability (variations around 3%). Instrument stability was evaluated with CO_2 measurements at a constant flow rate of 10 $Lmin^{-1}$ during 15 min. These measurements revealed constant values of scattering coefficients with differences below 1% versus theoretical values from (Bodhaine et al., 1991). Finally, inherent aspects of the imaging technique were evaluated such as the impact of the exposure time. The largest noise is found for exposure times below 5 s, while the smoother values are obtained for exposure times of 10-20 s. However, large exposure times can yield to more angles that are saturated, and the software must find a compromise between noise and saturation. Thus, the typical exposure time is of 10 s and with that we estimate that uncertainties in measured parallel and perpendicular signals are around 5% in laboratory conditions. The evaluation of the instrument versus known scattered (monodisperse polystyrene spheres - PSL) showed good agreements with RMSE around 0.10 for both F_{11} and $-F_{12}/F_{11}$.

The uncertainties in direct measurements of the instrument (parallel and perpendicular signals) under laboratory conditions imply uncertainties below 10% in F_{11} and below 20% in $-F_{12}/F_{11}$. However, in-situ measurements present natural variability of the aerosol sampled and the differences can be enhanced because of the short exposure times (~ 10s). Effects during the measurements such as saturation or low signal to noise ratios (SNR) of some pixels can happen. Other issues such as the passage of an individual

super-coarse particle can have an impact on certain angles of the phase matrix. Therefore, we apply a data-quality check procedure that accounts for all these issues and provide an effective phase matrix representative of an average time of 30 min or 1 hour, depending on the specific conditions of natural aerosol variability. Note that standard deviations during these periods might be larger than the uncertainties of the instrument. Details of this quality check procedure are in Bazo et al., (2024)."

In Tab. 2 you don't provide any uncertainties at all. Please add them.

-Thanks for pointing this out. In the revised manuscript we include now the standard deviations of the hourly means in Table 2, as a representation of the variability of the aerosol particles being sampled. We have also added in the Table caption that error bars are the standard deviations of the hourly means (L589):

"Error bars are the standard deviations of the hourly means."

Your phase matrix elements (Fig. 6,7 & 9) do not contain any uncertainties. Putting an error bar to every point would certainly overload the figure, but having at least 3 points with error bars in each plot would help to assess the range of uncertainty.

We thank the referee for the suggestion. In Figure R5 we show some examples of the hourly phase function and polarized phase function with the standard deviation as error bars in several angles, including angles in the forward (~5-10º) and backward (~150-175º) scattering as well as in the middle (~90-100º) of the angular range. We have chosen to represent the standard deviation of the hourly averages because these values are larger than the uncertainty of the instrument. However, one must keep in mind that these standard deviations represent the variability of the different parcels of air that are being sampled throughout the hour, and they are not in any way uncertainty of the PI-Neph's measurements. We observe that for less variable conditions, such as a clean atmosphere or a highly polluted atmosphere, the standard deviations are smaller than those obtained during situations when the air is changing. In any case, the standard deviation in the phase functions is around 20% of the hourly mean, whereas for the $-F_{12}/F_{11}$ element the values of the standard deviations are more variable, usually ranging from 0.05-0.1 in the forward region and 0.1-0.2 in the other regions.

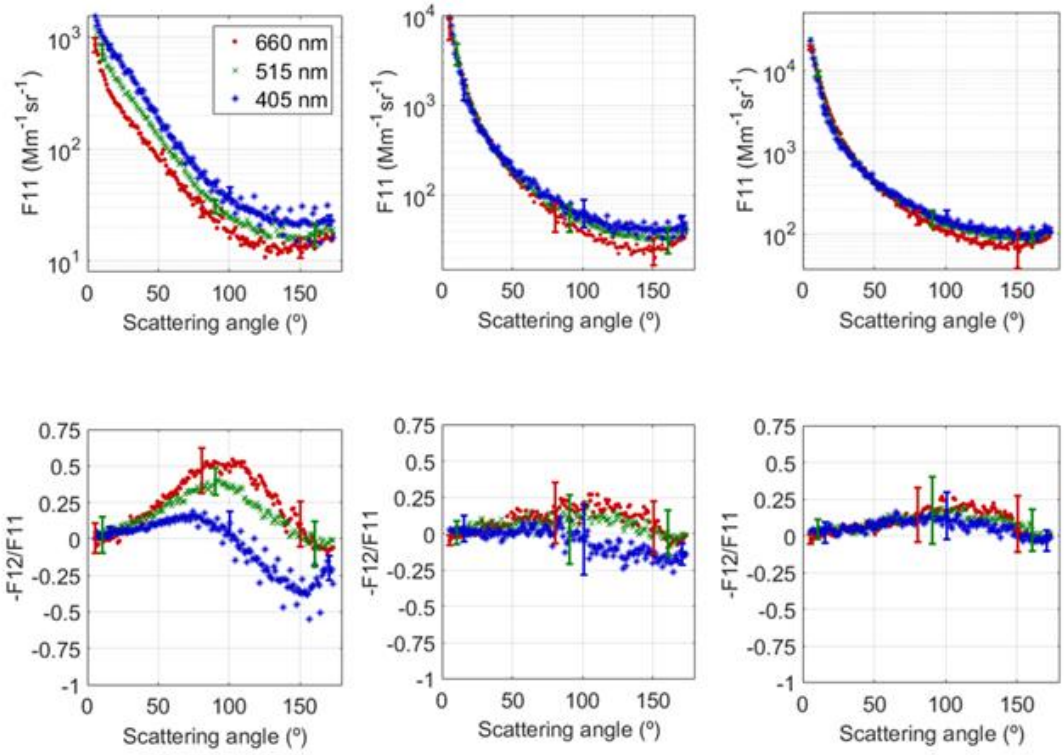

Figure R5. Examples of hourly phase functions (F11, top) and polarized phase functions (-F12/F11, bottom) with the standard deviation as error bars.

As already mentioned, the standard deviations in the scattering matrix elements are only a representation of the variability of the atmosphere that surrounds the sampling line connected to the instruments. Therefore, since it does not represent the uncertainty of the measurements, we have not added any error bars to Figures 6,7 and 9. We refer to the reader to our previous study (Bazo et al., 2024) where we evaluated the performance of the instrument and studied its sources of error (see modified text in previous comment) in laboratory under controlled conditions.

And we have also indicated the usual range of variability of the scattering matrix elements shown in this work (L415-L419):

"Computed standard deviations were larger than instrument uncertainties and they are associated with the variability of the different parcels of air sampled throughout the hour of measurements. These standard deviations were of ~ 20% for F_{11} and ranging between 0.1 and 0.2 for $-F_{12}/F_{11}$ (minimums for the forward region and maximums in the middle region around 90º)."

L463-L465: "Again, the computed standard deviations are larger than the uncertainties of the instruments and they represent the variability of the samples. As for the previous extreme event, these standard deviations are ~20% for F_{11} and between 0.1- 0.2 for $-F_{12}/F_{11}$. "

L568-L570: "The standard deviations were 20-30% for F_{11} and around 0.2 in $-F_{12}/F_{11}$, which are larger than the uncertainties of the instruments for all cases and explained by the large variability of aerosol samples during the measurement process"

4. After finalizing my review, I am now reading the comments of Jean-Baptiste Renard and I want to enforce his point, that the (spectral) scattering properties depend on particle size (see my major comment #2). And there is much more literature on the size effect of the polarized scattering properties than mentioned in his comment. The size effect is almost not discussed in the manuscript. Please try seriously to get more size information than just a PM10 concentration.

We agree with the referee and with Dr. Jean-Baptiste Renard. Without information of size distribution, we have to be cautious in the interpretation of our results. As commented above, correlative measurements of aerosol size distributions were not available specially during the two extreme Saharan dust outbreaks. In the LUMINOUS field campaign, we are acquiring such kind of correlative data polarized polar nephelometry + size distributions + chemical information.

After reading all the issues raised by the referees, we believe that we have been naive in the interpretation of the phase matrix results. The patterns observed can be associated with many causes – differences in the size distribution, size of particles and refractive indexes – that were not measured correlatively. This is even more complicated when we study mixtures of different particles. In the revised manuscript we have avoided any hypothesis and remark that further correlative measurements are needed.

In the conclusion section, we insist that our novelty is on the measurement of phase matrix elements of ambient aerosols, and that we present some of the first measurements for ambient Saharan dust (L772-L785).

"This work has focused on the analyses of aerosol phase matrix elements and other optical properties during Saharan dust outbreaks that were registered in the UGR station (Southeastern Spain) in the year 2022. The main novelty of the analyses are the measurements by the multiwavelength Polarized Imaging Nephelometer (PI-Neph) developed by GRASP-Earth and capable of providing two aerosol scattering matrix elements (F_{11} and $-F_{12}/F_{11}$) for three different wavelengths (405, 515 and 660 nm). The uniqueness of PI-Neph is that it allows to measure phase matrix elements of ambient aerosol. The instrument can provide F_{11} and $-F_{12}/F_{11}$ with 10% and 20% uncertainty, respectively, under laboratory conditions. The optimization of the instrument and the use of appropriate data quality check approach served to continuously measure F_{11} and $-F_{12}/F_{11}$ for ambient air, but in these cases the natural variability of the air sampled typically imply large uncertainties, being the typical standard deviations of ~20% for F_{11} and between 0.1- 0.2 for $-F_{12}/F_{11}$ and therefore larger than the uncertainties of the instrument. The multiwavelength F_{11} and $-F_{12}/F_{11}$ measurements for different Saharan dust outbreaks are some of the first carried out for ambient aerosols and serve to complement laboratory measurements of mineral dust particles and of synthetic samples minerals that compose dust particles"

We also highlight that our measurements serve to complement other already measurements by in-situ and remote sensing instruments (L785-L789).

"The novel measurements of F_{11} and $-F_{12}/F_{11}$ can also complement other optical and microphysical properties of Saharan dust already known from in-situ instrumentation and by active and passive remote sensing instruments, both from the ground and the space.

Nevertheless, more F_{11} and $-F_{12}/F_{11}$ measurements are needed at other experimental sites to have a more complete vision of mineral dust role on climate."

And we remark that further experiments are needed combining PI-Neph with other instruments that provide chemical information and size distribution of aerosol particles (L860-L864).

"However, going further in understanding the interaction of dust with these anthropogenic particles requires further analyses that provide the chemical composition and size distribution of the ensemble of particles and the final composition and shape of the particles after interacting. This is planned in future studies that will allow a more complete comprehensive analysis."

Minor comments:

- **Title: "polarized polar imaging nephelometry" – in the manuscript, you always state Polarized Imaging Nephelometer (PI-Neph). Why do you use the term "polar" only in the title?**

-Thanks for the suggestion. The name of the instrument is as written in the manuscript (Polarized Imaging Nephelometer), but we wanted to highlight the angular resolution of the instrument in the title, so we added the term polar to it.

- **L20 Please mention already in the introduction the angular range of the instrument.**

-Done.

- **L56 a strange unit.**

-We refer to the inverse of the climate sensitivity parameter, which expresses the change in temperature per unit of radiative forcing. We have changed the notation of the units in the main text to make it clearer.

- **L67 complex refractive index**

-Thanks. It has been corrected.

- **Your introduction (L70-85) is focused on passive remote sensing. I am missing the active remote sensing with e.g., CALIPSO or EarthCARE and the linked laboratory studies which focus on the backscattered light close to 180° (e.g., Sakai et al., 2010, Järvinen et al., 2016 or Miffre et al., 2023).**

We thank you for this suggestion. We have modified the introduction to better contextualize our work (see major comment above). For space measurements, polarization only affects the retrieval of aerosol properties for space polarimetry and that has been stated in the revised introduction. Including references to EarthCare or CALIPSO would have made the introduction more confusing because PI-Neph does not provide measurements at 180º that is the angle required for lidar measurements. In Section 2.2.2 where we explain how to compute the LRs we mention that PI-Neph is not the ideal instrument to measure LRs. Indeed, other instruments are more appropriate (L268-L270):

"We highlight that PI-Neph is not designed to accurately measure $F_{11}(180º)$ and there are other specific instruments that serve for that purpose (Järvinen et al., 2016; Miffre et al., 2023; Sakai et al., 2010)."

We have also highlighted in the conclusion section that PI-Neph measurements serve to complement other measurements from in-situ instrumentation and by active and passive remote sensing instruments (L785-L788):

"The novel measurements of F_{11} and $-F_{12}/F_{11}$ can also complement other optical and microphysical properties of Saharan dust already known from in-situ instrumentation and by active and passive remote sensing instruments, both from the ground and the space."

- **Eq 5 + 6: Do you use the decadic logarithm (log) or the natural logarithm (ln) for your definition?**

-Thanks for pointing this out. We use the natural logarithm; we have changed the notation in equations 5 and 6.

- **According to eq. (7), the units of the LR should be sr and not sr-1. Please change it throughout the manuscript (including figures and tables).**

-We thank the reviewer for identifying this mistake, we have changed it throughout the manuscript and in the figures and tables.

- **How do you extrapolate to the scattering angle of 180°. Please add some description and assessment of the related uncertainties.**

-The objective is not to compute $F_{11}(180°)$. Indeed, we want to estimate F_{11} for the range 175º - 180º. To do so we used methodology based on linear extrapolation using the neighbors measurements. According to studies of Horvath et al., (2015), these linear extrapolations only imply 5% uncertainty in the computation of σ_{sca}, g and B_s. We have modified the text to clarify this point (L234-L235):

"… where data from 0 to 5° and from 175 to 180° have been linearly extrapolated to obtain the complete phase function which according to Horvath, (2015) only implies uncertainties up to 5% in the computations of the σ_{sca}, g and B_s. "

- **From the reader's perspective, I would suggest a different section numbering to avoid the 4th level of subsections (e.g., 3.2.1.1). My suggestions are: Give the meteorological conditions (currently Sect. 3.1) an own section (Sect. 3) before you go to your results of the PI-Neph in Sect. 4 (Results or Aerosol phase matrix from different dust scenarios). Section 3.2.3 and 3.2.4 can be combined to new section: Sect. 5 – Discussion with 5.1 and 5.2 for the two respective subsections.**

We thank the referee for this feedback. We have re-shaped the manuscript in the following way:

Section 3 'Overview of extreme dust events during March 2022' that initially was sub-section 3.2.1.1. This section gives an overview of the meteorological conditions associated with these two extreme events, plus some satellite observations that give an overview of the intensity of the dust plume.

Section 4 ‘Results of aerosol phase matrix from different dust scenarios’: Here we include now sub-section 4.1 ‘Extreme events’ that was initially subsection 3.2.1.2, and sub-section 4.2 ‘Moderate dust events during spring/summer 2022’ that was initially subsection 3.2.2

Section 5 ‘Discussion’: Here we include the sub-section 5.1 ‘Comprehensive assessment of the different dust events’ that initially was sub-section 3.2.3 and sub-section 5.2 ‘Phase matrix simulations for different aerosol mixture scenarios’ that initially was sub-section 3.2.4

- **The meteorological conditions (Sect. 3.1) are given in great level of detail. I am wondering, if the 4 CAMS model outputs for each case are necessary, because this information is not used in the next sections. To my opinion, it can be combined to one CAMS output per dust case. In this section some lidar observations of the Granada station would be helpful to demonstrate the vertical layering of the dust above your station. It must not be a difference in the strength of the dust outbreak between the two cases in March, but on 15 March, the dust was mixed to a larger extend towards the ground and therefore to your PI-Nephelometer. Lidar observations would reveal the vertical layering of the dust.**

-We plotted the evolution of each event with the CAMS model in two separate graphs with the objective of illustrating the temporal evolution of the event and highlighting the moment of maximum intensity and spatial impact. We also analyzed the impact of the different events in terms of Aerosol Optical Depth measured by AERONET network.

The referee is right that lidar measurements would have given a great compliment. But as commented above, lidar measurements in the AGORA observatory were saturated in the first 1-2 km and did not fulfill the data-quality criterion of EARLINET/ACTRIS single calculus chain. Nevertheless, these measurements served as illustration that most transport of mineral dust during these events happened in the first 1-2 km, and that was added in the text (L334-L337):

“Lidar measurements at EARLINET\ACTRIS Granada station were saturated in the first 1-2 km and avoided any kind of retrieval of aerosol optical properties. Nevertheless, these measurements served to illustrate that most of the transport occurred in the first two kilometers above the ground.”

- **L200 Libya**

-Done.

- **L250 Please provide the values for usual dust outbreaks and not just a reference. Similarly, in line 373**

Thanks for the suggestion. This value is of ~100 μgm^{-3} and it is now specified in the revised manuscript.

- **Fig. 5 Please add more detailed steps to the time axis. The scale for SAE is not optimal.**

-Thanks for pointing this out. The axis and scale have been modified to make the Figure clearer.

- **L329-334 This text might be moved to the figure caption of Fig. 6. At least Fig. 6 needs some more explanations in the caption. The same holds for L 374-377 and Fig. 7.**

-We thank the referee for the suggestions. Figure 6 and Figure 7 captions have been modified in the revised manuscript:

L455-459: "Figure 6. Hourly averages of phase function (F_{11}) and polarized phase function ($-F_{12}/F_{11}$) on 15th - 16th March 2022 for four different stages of the evolution of the extreme Saharan dust outbreak: (a) 15th March 07:00 UTC before the Saharan dust outbreak reached the station, (b) 15th March 12:00 UTC when the Saharan dust begin to reach the station, (c) 15th March 17:00 UTC associated with the peak of the extreme Saharan dust intrusion, and (d) 16th March 13:00 UTC when Saharan dust start to withdrawn."

L493-497: "Figure 7. Hourly averages of phase function (F_{11}) and polarized phase function ($-F_{12}/F_{11}$) on 24th - 25th March 2022 for four different stages of the evolution of the extreme Saharan dust outbreak: (a) 24th March 13:00 UTC before the Saharan dust outbreak reached the station, (b) 24th March 21:00 UTC when the Saharan dust start to reach the station, (c) 25th March 09:00 UTC associated with the peak of the extreme Saharan dust outbreak, and 25th March 20:00 UTC when dust concentrations begin to withdrawn"

- **L340 "notable spectral separation" – I am not sure if it just a manner of scaling the y-axis. Fig. 6a1 has a maximum value of 10^3 whereas the other subfigures extend to 10^4. Therefore the spectral separation is better visible in Fig. 6a1.**

-The referee is right, the most remarkable spectral separation in F_{11} values is in Fig 6.a1. This point is even clearer if we make a zoom in Figure 6, as it is shown in Figure R6 showed below.

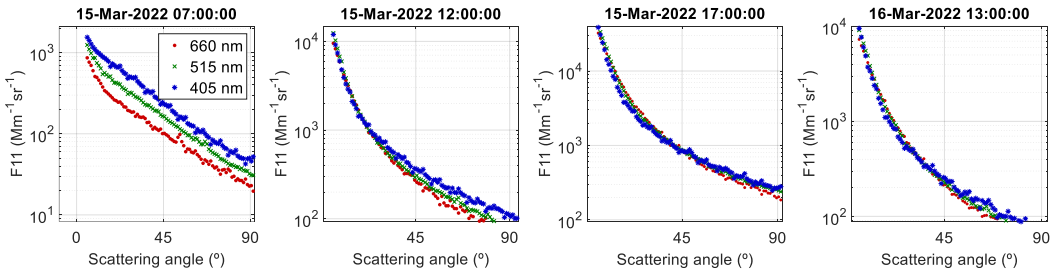

Figure R6. Zoom of the phase functions (F_{11}) for four different stages of the dust event on 15th-16th March 2022.

We therefore believe that our initial paragraph was not clear. That paragraph has been re-written to emphasize this point and avoid redundancies (L431-L442)

"Figure 6 shows a general pattern in F_{11} characterized by strong predominance of forward scattering up to two orders of magnitude greater than backward scattering. However, there are significant changes in both magnitudes and spectral dependence over time, that is, with the intensity of the dust outbreak passage. At the beginning of the dust event (Fig. 6a), the values of F_{11} in the forward scattering region are around 1000 $Mm^{-1}sr^{-1}$ for all

three wavelengths, which is even one order of magnitude lower when compared with the cases at the other moments of the event (i.e. 50000 $Mm^{-1}sr^{-1}$ for the three channels during the peak). Also, at the beginning of the event (Fig. 6a) notable spectral separation in F_{11} is observed while such spectral separation is negligible during the rest of the event when coarse mode particles largely predominate. All F_{11} show the minimum in the region 120º-140º but the magnitude of that minimum varies between the different stages. Also, around that minimum is the region where some spectral difference is observed during the cases of strong predominance of coarse mode (Fig. 6c-d). A recovery from that minimum is also observed, being more pronounced in cases close to the peak of the event."

- **Figs 6,7,9 lower row: the y-scaling is quite coarse, please add some ticks in between.**

-Done.

You may add the value of the PM10 concentration for the different time steps because you are discussing it a lot and it is not always visible from Fig. 5+8.

-We thank referee suggestion. This information can be found in Tables 1 and 2 and adding them could be repetitive.

The term "moment" seems not the best choice, maybe better "instances" or "time steps" or something else. Please consider changing it here and in the text.

-Done.

- **L381-383 Sentence unclear.**

-We have modified this sentence (L481-484).

"Figure 7 shows that F_{11} patterns are very similar to the previous extreme event on 15th - 16th March, with strong predominance of forward scattering (~25000 $Mm^{-1}sr^{-1}$), being two orders of magnitude above the backscattering (~100 $Mm^{-1}sr^{-1}$) at the peak of the event on 25th March 9:00 UTC. There are no significant spectral differences, as also happened for the other extreme event on 15th-16th March."

- **L387-389 Be more precise. The whole paragraph on page 11 needs some rephrasing to be more precise.**

-That paragraph has been re-written, and now is given by (L481-L491):

"Figure 7 shows that F_{11} patterns are very similar to the previous extreme event on 15th - 16th March, with strong predominance of forward scattering (~25000 $Mm^{-1}sr^{-1}$), being two orders of magnitude above the backscattering (~100 $Mm^{-1}sr^{-1}$) at the peak of the event on 25th March 9:00 UTC. There are no significant spectral differences, as also happened for the other extreme event on 15th-16th March. These patterns in F_{11} agree with laboratory measurements of dust samples (i.e. Muñoz et al., 2007; Renard et al., 2014; Volten et al., 2001). Nevertheless, there are some features in F_{11} with different situations: the slope in F_{11} in the forward scattering region becomes sharper when the PM_{10} concentrations are higher (Figs. 7b.1 and 7c.1). For the backward region F_{11} shows a flatter behavior for high PM_{10} concentrations (Figs. 7b.1 and 7.c.1), while for the cases with lower PM_{10} concentrations there is a sharp increase in scattering from 150° to 180°. During the

previous extreme dust outbreak, we observed flat patterns for the backward scattering region during the peaks of the dust intrusions."

- **Tab 1+2 "The angular range of the PI-Neph is used as the integration range of sigma_sca." Please provide the angular range otherwise this information is not very helpful.**

-We have added this information to the caption of the tables.

Why some values at 405 nm are missing on 25 March?

-After re-calculating using the data quality criterion in Bazo et al., (2024) we figure out that some data were eliminated incorrectly. Consequently, we have modified the values in Table 1 and Figure 5.

- **L450: A newer and more comprehensive overview of lidar ratios was reported in Floutsi et al., AMT 2023.**

-We thank the reviewer for this useful reference. We have added the citation in the text and included Floutsi et al., (2023) in the list of references.

- **Fig 8. Sorry, but it is really challenging to get anything out of Fig. 8. Please use more space to show your results, half of a page minimum. Or remove the figure from the manuscript. I see only dots and can hardly infer any value from the y-axis. You probably want to show that there are more dust outbreaks during summer.**

- We agree with the referee. We have used more space to show Figure 8.

- **Tab 2 and Fig. 9: Do you show the measurements for the whole day? Or for one hour? Or for the periods marked in Fig. 8?**

-We show hourly-averaged measurements that correspond to the peak in scattering during the dust event. We have added this information to the text (L567-568):

"Particularly, Fig. 9 shows hourly averages of F_{11} and $-F_{12}/F_{11}$ representative of the peak in scattering during each event."

- **Fig 10 and surrounding text: BC and BrC are not defined.**

-We have added the definitions of both acronyms in L625-626 following the definitions in Schmeisser et al. (2017).

"….where BC refers to black carbon and BrC to brown carbon in the definitions given by Schmeisser et al., (2017).

- **L539-541: Polarization measurements are very valuable for separating dust and non-dust contributions. This potential is used in the active remote sensing community for two decades now, starting with Shimizu et al., 2004, continuing to Tesche et al., 2009 and Mamouri and Ansmann 2017. You now adding PI-Nephelometer measurements to this separation.**

-We agree with the reviewer on this and we have accordingly modified the sentence (L646-647):

" …. show the potential of ground-based phase matrix measurements to distinguish between different types of aerosol mixtures."

- **Fig 11 Do you expect that the seasonal average of -F12/F11 should go back to zero for 180° or could it stay negative?**

-In Figure 11 we show F_{11} and $-F_{12}/F_{11}$ only in the range 5º-175º that are the ranges where the polar nephelometers operate. The value at 180º can be computed by linear extrapolation of the closest points (Horvath et al., (2015) or by other more complex methods such as the proposed in Gomez-Martin et al., (2021). However, the objective of this work is not to provide at the exact angle of 180º accurate values of F_{11} and $-F_{12}/F_{11}$, even though it is critical for the lidar community. What Figure 11 reveals is the larger standard deviations in the seasonal averages for scattering angles larger than 170º approximately when compared with the range 150-160º. Nevertheless, the standard deviations for scattering angles larger than 170º are lower than those standard deviations observed in the region of minimum $-F_{12}/F_{12}$ values. The standard deviations are explained because of the variability of the aerosol sampled during the entire season.

To clarify the issues related to the standard deviations in F_{11} and $-F_{12}/F_{11}$ patterns we have re-phrased the paragraph and now is given by (L683-692):

"Figure 11 shows that seasonal values of $-F_{12}/F_{11}$ present in all cases larger standard deviations when compared to F_{11}. Particularly, for 660 and 515 nm large standard deviations are found in the region between 50º-150º while for 405 nm the standard deviations are considerably lower. This suggests that these $-F_{12}/F_{11}$ values at 660 and 515 nm are very sensitive to changing conditions in the aerosol that is sampled. Moreover, the other region that presents remarkable standard deviations for all wavelengths is the region of scattering angles above 170º. That region is very sensitive to any change in particle type and size, what was demonstrated both from theoretical computations (Mischenko et al., 2002) and in laboratory measurements (Gomez-Martin et al., 2021). However, the lower standard deviations observed for the 405 nm wavelength indicate homogeneity in the response to polarization, even in the presence of other anthropogenic particles in the sample."

Please indicate the wavelengths for the Granada Amsterdam Light Scattering data base in the caption or even in the figure. By the way, 488 nm are much closer to 515 nm than to 405 nm. Why did you choose to show it together with the 405 nm?

-We have included the wavelengths for the Granada Amsterdam Light Scattering database in the caption and in the figure. We had compared the 488 nm wavelength with the 405nm to reinforce the fact that during the extreme dust events the 405nm in the PI-Neph shows similar results as other instruments in the laboratory. However, the reviewer is right about the wavelength difference. Therefore, we have also shown a comparison of the 488nm wavelength along with our measurements for 515 nm.

Yellow is probably not the best choice – could you choose a different color? And overall, the final publication should get the figure in a higher resolution. It is hard for me to distinguish the open circles from the stars.

-Thanks for the suggestion. We have changed the color of this dataset from yellow to light blue. Also, we have tried increasing the size of the markers in the figure. However, since the scattering matrix elements from the two extreme events are very similar, there is superposition of datasets, and we decided to keep the original sizes.

Caption: "top" instead of "up"

-Done.

- **Do you have a pure pollution case for comparison? It would certainly enhance the message to have a contrasting pollution case presented or repeated from Bazo et al., 2024 in this paper as well.**

-Unfortunately, for pure pollution we only have the case from Bazo et al., (2024).

- **Paragraph (L598-612): You already mentioned Teri et al., 2024. Here some more discussion to the polluted dust cases in the Eastern Mediterranean would be helpful. Overall, I would recommend placing your work in a broader context besides of previous measurements at Granada station.**

-The referee is right and a comparison with other places would have enriched the manuscript. But our paper focusses only on F_{11} and $-F_{12}/F_{11}$ from ambient air, and unfortunately, we are not aware of the availability of other studies in the Eastern Mediterranean that deal with this type of measurements. Referee 1 pointed out that conclusions cannot be extrapolated to all kinds of mineral dust particles, with is very interesting point as well. Therefore, we have modified the conclusion section remarking that more measurements at other experimental sites are needed (L785-L789).

"…The novel measurements of F_{11} and $-F_{12}/F_{11}$ can also complement other optical and microphysical properties of Saharan dust already known from in-situ instrumentation and by active and passive remote sensing instruments, both from the ground and the space. Nevertheless, more F_{11} and $-F_{12}/F_{11}$ measurements are needed at other experimental sites to have a more complete vision of mineral dust role on climate."

- **L654-657: Sentence unclear. Please rephrase to be more precise.**

-Thanks for the feedback. In the revised manuscript it is now written (L766-L768):

"Future optimization in GRASP will permit the retrieval of aerosol refractive indexes between fine and coarse mode separately using as inputs F_{11} and $-F_{12}/F_{11}$, and thus permitting further analyses of the different study cases discussed in this work"

- **Fig. 12 The negative values for the $-F_{12}/F_{11}$ close to 180° for the pure dust case are not seen in the observations of the extreme dust events. Is it a modelling artefact or is it missing in the observations? What is your explanation? Please discuss in your paper.**

-We are not sure we understand this point. Figure 12, which are GRASP simulations, shows negative values of $-F_{12}/F_{11}$ very close to zero in the backward scattering region. If the reviewer refers to the observations from Figure 11, we include below a zoom close to 180º region (Figure R7). We can observe values very close to zero in $-F_{12}/F_{11}$ for scattering angles close to 180º - any difference falls within the uncertainties. Note that theoretically

$-F_{12}/F_{11}$ is zero only under the assumption of mirror symmetry and randomly oriented particles in the sample, that is not always fulfilled in the nature (Mischenko et al., 2002). We also observe a small negative branch of $-F_{12}/F_{11}$ near 180º, as the simulations from Figure 12 showed.

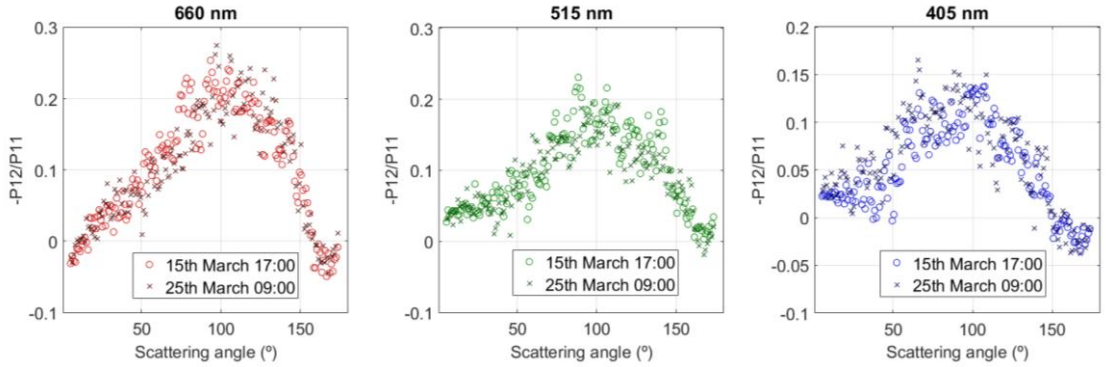

Figure R7. Zoom of the degree of linear polarizations ($-F_{12}/F_{11}$) for the extreme events in March 2022.

We have included the following statement (L755-757):

"…with small negative values around 180º. Note that this feature is also present in the $-F_{12}/F_{11}$ in Figure 11 for the extreme dust cases, but it is not noticeable due to the scale."

- **L668: "To our knowledge, these are the first measurements of this type for ambient mineral dust transported to southern Europe" – only in Southern Europe. Where else ambient mineral dust measurements have been performed? What is the difference to your observations?**

-We are referring to F_{11} and $-F_{12}/F_{11}$ measurements of ambient mineral dust. Previous study of Horvath et al., (2018) measured F_{11} with a single-wavelength polar nephelometer of ambient transported Saharan dust aerosol in the Sierra Nevada National Park, which is around 20 km in horizontal distance from the UGR station where the measurements in this work took place. However, this study did not provide multiwavelength $-F_{12}/F_{11}$ measurements.

On the other hand, previous designs of PI-Neph by the University of Maryland, Baltimore County (UMBC) provide the F_{11} and $-F_{12}/F_{11}$ measurements of ambient aerosol. In the DC3 field campaign the first design of PI-Neph operated only at 532 nm, while in SEAC4RS it operated with 473, 532 and 671 (Espinosa et al., 2017, 2018, 2019). Another PI-Neph version (also developed in UMBC) can acquire F_{11} and $-F_{12}/F_{11}$ measurements at 660 and 405 and is operated by NOAA (Ahern et al., 2022). However, these instruments have not acquired multiwavelength measurements of Saharan dust yet. There are other developments in laser imaging nephelometry (i.e Moallemi et al., 2023) capable of measuring F_{11} and $-F_{12}/F_{11}$ but up to now these instruments only operate for laboratory conditions. All these issues are now included in the new instruction section (L129-L146):

"The latest developments use imaging techniques (Bian et al., 2017; Curtis et al., 2007; Dolgos & Martins, 2014a) to determine phase matrix with single detector and relatively compact design that does not require moveable parts. The Polarized Imaging Nephelometer (PI-Neph) was one of the first designs of a polar nephelometer that used imaging techniques, developed by the University of Maryland, Baltimore County

(UMBC). This first prototype of the PI-Neph was capable of acquiring aerosol phase matrix at 473, 532 and 671 nm with 0.5º resolution. The instrument was deployed on the NASA DC8 aircraft and operated during special field (Espinosa et al., 2018; Reed Espinosa et al., 2017). Other PI-Neph instruments based on the first UMBC design are operated by NOAA (Ahern et al., 2022; Manfred et al., 2018). The main novelty of these prototypes is that they measure phase matrix elements of ambient air, when conditions can be very different to laboratory measurements. However, to date none of these instruments have been operating continuously and report any multiwavelength measurements of Saharan dust. The imaging technique is being expanded worldwide with further designs although limited to laboratory operation yet (Moallemi et al., 2023). All designs in polar nephelometry present physical limitations that limit the measurements to the range 3º-178º, but synthetic tests have revealed that multi-wavelength polarimetric PI-Neph measurements improve the information content for the retrieval of aerosol optical and microphysical properties (Moallemi et al., 2022) . Therefore, measurements of dust phase matrix elements for ambient aerosol samples in the atmosphere will serve to advance in the understanding of mineral dust absorption properties and chemical composition (Di Biagio et al., 2017, 2019)."

We personally are very cautious in claiming the first of doing something, and by that end we have modified the sentence claiming the novelty of our measurements and highlighting the complement with other measurements. The sentence in the new conclusions section is now given by (L785-L789):

"The novel measurements of F_{11} and $-F_{12}/F_{11}$ can also complement other optical and microphysical properties of Saharan dust already known from in-situ instrumentation and by active and passive remote sensing instruments, both from the ground and the space. Nevertheless, more F_{11} and $-F_{12}/F_{11}$ measurements are needed at other experimental sites to have a more complete vision of mineral dust role on climate."

References added:

Ahern, A. T., Erdesz, F., Wagner, N. L., Brock, C. A., Lyu, M., Slovacek, K., Moore, R. H., Wiggins, E. B., & Murphy, D. M. (2022). Laser imaging nephelometer for aircraft deployment. *Atmospheric Measurement Techniques*, *15*(5), 1093–1105. https://doi.org/10.5194/amt-15-1093-2022

Bian, Y., Zhao, C., Xu, W., Zhao, G., Tao, J., & Kuang, Y. (2017). Development and validation of a CCD-laser aerosol detective system for measuring the ambient aerosol phase function. *Atmospheric Measurement Techniques*, *10*(6), 2313–2322. https://doi.org/10.5194/amt-10-2313-2017

Curtis, D. B., Aycibin, M., Young, M. A., Grassian, V. H., & Kleiber, P. D. (2007). Simultaneous measurement of light-scattering properties and particle size distribution for aerosols: Application to ammonium sulfate and quartz aerosol particles. *Atmospheric Environment*, *41*(22), 4748–4758. https://doi.org/10.1016/j.atmosenv.2007.03.020

Manfred, K. M., Washenfelder, R. A., Wagner, N. L., Adler, G., Erdesz, F., Womack, C. C., Lamb, K. D., Schwarz, J. P., Franchin, A., Selimovic, V., Yokelson, R. J., & Murphy, D. M. (2018). Investigating biomass burning aerosol morphology using a laser imaging

nephelometer. *Atmospheric Chemistry and Physics*, *18*(3), 1879–1894. https://doi.org/10.5194/acp-18-1879-2018

- **L691 versus --> to**

-Done.

- **L699 SSA and LR are intensive properties**

-This was a typo, thank you for pointing it out.

- **The author's contributions section is missing.**

-We have added this section between L866 and L872:

"EB analyzed the data and wrote the manuscript. DPR defined the structure of the paper, conceptualized the investigation and supervised the writing of the manuscript. ADZ analyzed the meteorological conditions during the extreme Saharan dust outbreaks. FR performed the GRASP simulations. FJO, AV and LAA are the principal investigators of the projects that funded the research and put the guidelines of the research. GT, AC, DP, FJGI assisted in the conceptualization. JVM and DF contributed to the development of the instrumentation. All authors contributed to the discussion of the results and provided comments on the paper."

References:

Järvinen, E.; Kemppinen, O.; Nousiainen, T.; Kociok, T.; Möhler, O.; Leisner, T. & Schnaiter, M.: Laboratory investigations of mineral dust near-backscattering depolarization ratios, Journal of Quantitative Spectroscopy and Radiative Transfer, 2016, 178, 192 – 208.

Floutsi, A. A.; Baars, H.; Engelmann, R.; Althausen, D.; Ansmann, A.; Bohlmann, S.; Heese, B.; Hofer, J.; Kanitz, T.; Haarig, M.; Ohneiser, K.; Radenz, M.; Seifert, P.; Skupin, A.; Yin, Z.; Abdullaev, S. F.; Komppula, M.; Filioglou, M.; Giannakaki, E.; Stachlewska, I. S.; Janicka, L.; Bortoli, D.; Marinou, E.; Amiridis, V.; Gialitaki, A.; Mamouri, R.-E.; Barja, B. & Wandinger, U.: DeLiAn -- a growing collection of depolarization ratio, lidar ratio and Ångström exponent for different aerosol types and mixtures from ground-based lidar observations, Atmospheric Measurement Techniques, 2023, 16, 2353-2379.

Mamouri, R.-E. & Ansmann, A.: Potential of polarization/Raman lidar to separate fine dust, coarse dust, maritime, and anthropogenic aerosol profiles, Atmospheric Measurement Techniques, 2017, 10, 3403-3427.

Miffre, A.; Cholleton, D.; Noël, C. & Rairoux, P.: Investigating the dependence of mineral dust depolarization on complex refractive index and size with a laboratory polarimeter at 180.0degree lidar backscattering angle, Atmospheric Measurement Techniques, 2023, 16, 403-417.

Sakai, T.; Nagai, T.; Zaizen, Y. & Mano, Y.: Backscattering linear depolarization ratio measurements of mineral, sea-salt, and ammonium sulfate particles simulated in a laboratory chamber, Appl. Opt., OSA, 2010, 49, 4441-4449.

Shimizu, A.; Sugimoto, N.; Matsui, I.; Arao, K.; Uno, I.; Murayama, T.; Kagawa, N.; Aoki, K.; Uchiyama, A. & Yamazaki, A.: Continuous observations of Asian dust and other aerosols by polarization lidars in China and Japan during ACE-Asia, Journal of Geophysical Research: Atmospheres, 2004, 109, D19S17.

Tesche, M.; Ansmann, A.; Müller, D.; Althausen, D.; Engelmann, R.; Freudenthaler, V. & Gross, S.: Vertically resolved separation of dust and smoke over Cape Verde using multiwavelength Raman and polarization lidars during Saharan Mineral Dust Experiment 2008, Journal of Geophysical Research: Atmospheres, 2009, 114, D13202.